RSC Advances

ROYAL SOCIETY OF CHEMISTRY

www.rsc.org/advances

RCS Advances

ARTICLE

Eutectic Ionic Liquid mixtures and its effect on CO_2 solubility and conductivity

-Received 00th January 20xx,
Accepted 00th January 20xx

DOI: 10.1039/x0xx00000x

www.rsc.org/

Anna S. Ivanova,[a] Thomas Brinzer,[b] Elliot A. Roth,[d] Victor A. Kusuma,[d] John D. Watkins,[d] Xu Zhou,[d,c] David Luebke,[d] David Hopkinson,[d] Newell R. Washburn,[a] Sean Garrett-Roe,[b]† Hunaid B. Nulwala[a,d]†

A simple binary system of compounds resembling short-chain versions of popular ionic liquids has been shown to have surprisingly complex properties. Combining methylated versions of pyridinium and pyrrolidinium bis[(trifluoromethyl)sulfonyl]imide accesses desirable properties such as low viscosity, high conductivity, and high CO_2 solubility per unit volume was acheived. The binary combinations studied in this study showed that these materials were stable liquids at 50°C and had is a threefold improvement in conductivty over [C_6C_1im][Tf_2N]. Despite their high densities, 2D-IR studies indicate increased ion mobility, likely due to the lack of hindering alkyl chains.

Introduction

Ionic liquids (ILs) have a potential advantage over existing solvents as a green medium due to their wide liquid range, outstanding solvation potential, negligible vapour pressure, thermal stability, and recyclability.[1–3] These properties have prompted their use as lubricants, electrolytes for energy storage, CO_2 capture media, coatings, and fuel cells.[4–7] However, the optimization of IL properties for a given application is a challenge. Through skilful manipulation of IL structures, one can target specific properties such as viscosity, solubility, conductivity, melting point, density, refractive ind[6,8–12] principle, one can design novel ILs with the exact properties needed, but in practice, this is a daunting goal to achieve.

ILs are complex solvents, whose properties ultimately depend on multiple intermolecular forces, including hydrogen bonding, ionic/charge–charge, dipolar, π–π, n–π, and van der Waals interactions. These interactions are large and quite complex when compared to simple solvents. Thus, it is difficult to tune the properties of ILs without extensive synthetic manipulations and careful characterization. One simple, alternate route to access specific properties is by creating mixtures of ILs.[13,14] The properties of IL mixtures have been shown to be distinct from those of the parent compounds and researchers have started to evaluate the mixture of binary and ternary mixture.[15–24] The mixing of ILs can lead to improve liquid range and compound various properties of ILs. Ionic materials having melting points over 100°C have not been extensively studied and there remain an opportunity to further extend the useful properties.[23] The exception is work by maximo et al.[23] who has studied the melting behaviour of ionic solids mixtures.

Ionic solids are crystalline material with higher density. Like normal salts, these organic solids show eutectic behaviour upon mixing. In our work various compositions of mixtures combining 1,1-dimethylpyrrolidinium and 1-methylpyridinium and bis[(trifluoromethyl)sulfonyl]imide (Both are solids and crystalline materials at room temperature) ($[C_1C_1pyrr]_x[C_1pyr]_{(1-x)}[Tf_2N]$) (The subscripts show the mole fraction) (Figure 1) were studied. This combination is unusual because it lacks the bulky alkyl chain normally used to disrupt crystal lattice packing and lower the melting points of traditional ILs. Also the anion is not symmetrical unlike the study done previously. The pristine ionic salts are crystalline solids with sharp melting transitions.

Typically, ILs rely on molecular asymmetry to disrupt the crystalline ordering of the ions and widen the liquid range.[25] With symmetric cations, this effect must be achieved by other means. By combining two cations with different electronics or crystal phase, we aimed to introduce defects into the molecular ordering and induce a eutectic effect, resulting in a lower melting point.[14] Additionally, the shortened alkyl chains should eliminate the problem of tail group domains causing spatial heterogeneity,[26] potentially increasing the rate of diffusion through the IL and, thus, improving the kinetics of gas adsorption.[27] Though gas solubility is known to generally increase with the size and flexibility of ionic structures, for CO_2 the dominant effect is gas–anion interaction.[28] Finally, the decreased cation size should increase the charge density of the mixture, possibly improving conductivity. Thus, the

[a] Department of Chemistry, Carnegie Mellon University, 4400 Fifth Avenue, Pittsburgh, PA 15213.
[b] University of Pittsburgh, Department of Chemistry, Chevron Science Center, 219 Parkman Avenue Pittsburgh, PA 15260.
[c] Liquid Ion Solutions, LLC. 1817 Parkway View Drive, Pittsburgh PA 15205.
[d] National Energy Technology Laboratory, P.O. Box 10940, Pittsburgh, Pennsylvania 15236.
† Corresponding authors—Hunaid Nulwala: E-mail: hnulwala@andrew.cmu.edu; Sean Garrett-Roe: E-mail: sgr@pitt.edu

combination $[C_1C_1pyrr]_x[C_1pyr]_{(1-x)}[Tf_2N]$ should result in a low-melting, conductive mixture with good gas solubility, making it widely applicable.

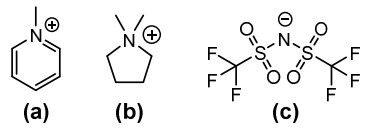

Figure 1. Components of synthesized compounds: a) 1-methylpyridinium cation [C_1pyr]; b) 1,1-dimethylpyrrolidinium cation [C_1C_1pyrr]; c) bis((trifluoromethyl)sulfonyl)imide anion [Tf_2N].

Experimental

Synthetic Details

[C_1C_1pyrr][I]

Pyridine (8.2 mL, 101 mmol) was stirred into acetonitrile (50 mL) at room temperature in air. The solution was cooled in an ice/water bath while slowly adding methyl iodide (7.6 mL, 121 mmol). The resulting clear yellow solution was allowed to warm to room temperature and stirred for 7.5 hours. Diethyl ether (~40 mL) was added, resulting in precipitation of a white powder. This product was collected on a fine sintered glass frit and rinsed three times with diethyl ether. A second batch of precipitate was collected from the filtrate and combined with the first. This solid was then dried in vacuo, yielding a white powder with a faint yellow tinge as a crude product (22.16 g, 100 mmol, 99.3%). ^{1}H NMR (300 MHz, $(CD_3)_2SO$): δ 9.00 (d, 2H), 8.59 (t, 1H), 8.14 (t, 2H), 4.36 (s, 3H).

[C_1C_1pyrr][Tf_2N]

A solution of lithium bis[(trifluoromethyl)sulfonyl]imide (31.79 g, 111 mmol) in water (50 mL) was added to a solution of 1-methylpyridinium iodide (22.16 g, 100 mmol) in water (35 mL) at room temperature in air. The resulting mixture of colorless liquid and white precipitate was stirred for 2 hours, then the solid product was collected on a fine sintered glass frit and rinsed three times with water. This white powder was then dissolved in ethyl acetate (~50 mL) and washed with an equivalent amount of water, shaking gently to avoid emulsion. The organic layer was collected and dried with $MgSO_4$, then solvent was removed by rotary evaporation, yielding a white powder (24.41 g, 65.2 mmol, 65.0%). ^{1}H NMR (300 MHz, $(CD_3)_2SO$): δ 8.98(d, 2H), 8.57 (t, 1H), 8.13 (t, 2H), 4.35 (s, 3H). ^{13}C NMR (300 MHz, $(CD_3)_2SO$): δ 146.0, 145.5, 128.1, 119.9 (q), 48.4. ^{19}F NMR (300 MHz, $(CD_3)_2SO$): δ 78.7.

[C_1pyr][I]

1-methylpyrrolidine (10.4 mL, 99.8 mmol) was stirred into acetonitrile (50 mL) at room temperature in air. The solution was cooled in an ice/water bath while slowly adding methyl iodide (7.5 mL, 120 mmol). The resulting cloudy white mixture was allowed to warm to room temperature and stirred for 7.5 hours. Diethyl ether (~50 mL) was added to complete precipitation. This product was collected on a fine sintered glass frit and rinsed three times with diethyl ether. A second batch of precipitate was collected from the filtrate and combined with the first. This solid was then dried in vacuo, yielding a white powder with a yellow tinge (20.73 g, 91.3 mmol, 91.5%). ^{1}H NMR (300 MHz, $(CD_3)_2SO$): δ 3.47 (m, 4H), 3.10 (s, 6H), 2.10 (m, 4H).

[C_1pyr][Tf_2N]

A solution of lithium bis[(trifluoromethyl)sulfonyl]imide (31.06 g, 108 mmol) in water (70 mL) was added to a solution of 1,1-methylpyrrolidinium iodide (22.33 g, 98.3 mmol) in water (20 mL) at room temperature in air. The resulting mixture of colorless liquid and white precipitate was stirred for 2 hours, then the solid product was collected on a fine sintered glass frit and rinsed three times with water. This white powder was then dissolved in dichloromethane and washed with an equivalent amount of water, shaking gently to avoid emulsion. The organic layer was collected and dried with $MgSO_4$, then solvent was removed by rotary evaporation, yielding a white powder (24.85 g, 65.3 mmol, 66.5%).

Note: All compounds were tested with Aq silver nitrate (1 M) solution. No visible silver halide formation was observed.

Experimental details are provided in the supporting material.

Results and Discussion

Melting behaviour

Melting point and thermal stability were used as an initial screening methodology. Thermal stability was determined by using thermogravimetric analysis (TGA) to identify the onset temperature of decomposition for each sample. In all cases, the onset point was above 415°C with a ramp rate of 10°C/min representing a ~65°C improvement over typical IL decomposition temperatures. This improvement is due to the removal of alky chain length which would decompose first compared to the rest of the molecule mainly due to the presence of alpha and beta protons. The absence of the alkyl chain lengths would also result in higher ionicity and conductivity thus improving the overall stability. The melting points were obtained by differential scanning calorimetry (DSC) using a 10°C/min ramp rate and were plotted to observe the effect of sample composition on melting temperature (Figure 2). We also performed modulated DSC experiments on 3 samples found no deviation from normal DSC in this case. In cases where multiple peaks were observed, the highest-temperature peak was assumed to be the melting point, ensuring a fully liquid sample. Nevertheless, the multiphasic behaviour of such samples indicates potential plastic[29] or liquid crystal[30] properties and is worth further exploration for electrolytic applications. The lowest melting point of the combinations is observed for $[C_1C_1pyrr]_{0.3}[C_1pyr]_{0.7}[Tf_2N]$, which exhibits a shallow eutectic point of 33.0°C. In total, four samples ranging from 0–30% [C_1C_1pyrr][Tf_2N] were completely liquid below 50 °C. We focused on analysing the CO_2 capture properties of these low-melting candidates.

Interestingly, the pyridinium parent compound and several of the binary combinations exhibit a strong supercooling effect, with crystallization occurring as much as 60 °C below the

melting temperature. These samples were meta-stable liquids at room temperature unless crystallization was seeded or initiated through mechanical forces, at which point rapid crystallization was observed. Such behaviour suggests a kinetically hindered nucleation step in the pyridinium compound, possibly exacerbated in the mixtures due to the complex stacking interactions of multiple cations.

Viscosity

Low viscosity of the IL is responsible for enhancing kinetics in gas capture and reaction media. Viscosities were measured at 50°C for the low-melting samples (Table 1). 1-hexyl-3-methylimidazolium bis[(trifluoromethyl)sulfonyl]imide, or $[C_6C_1im][Tf_2N]$ is used as a baseline standard for efficacy of other ILs[20,31,32] and has been selected as a reference ionic liquid for an IUPAC experimental validation project. It has a melting point of -7°C.[18] At 50°C, the viscosity of $[C_6C_1im][Tf_2N]$ is 26 mPa·s. Which is higher than most of our low-melting candidates at 50°C. Though the melting temperature steadily decreases from 0–30% $[C_1C_1pyrr][Tf_2N]$, the viscosity increases along the series. This unexpected trend suggests that the individual components are more important in determining viscosity than proximity of measuring temperature to melting point.

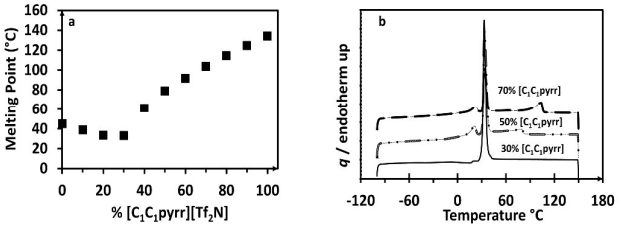

Figure 2. a) DSC heating curves of $[C_1C_1pyrr]_{0.3}[C_1pyr]_{0.7}[Tf_2N]$ (solid), $[C_1C_1pyrr]_{0.5}[C_1pyr]_{0.5}[Tf_2N]$ (short dashes), and $[C_1C_1pyrr]_{0.7}[C_1pyr]_{0.3}[Tf_2N]$ (long dashes) b) Melting points of binary combinations of ILs measured by DSC with a 10°C heating rate.

CO_2 uptake and density

The densities of the samples at 50°C are all significantly above those of $[C_6C_1im][Tf_2N]$, as expected for a system involving small, symmetrical cations and the lack of alkyl chains (Table 1). A slight decrease in density as the fraction of $[C_1C_1pyrr][Tf_2N]$ increases was noted, which can be explained by the increased proportion of pyrrolidinium cations interfering with orderly stacking.

Intuitively, high density should cause less free volume and reduce CO_2 uptake.[33] We find, however, that the increase in ionic concentration improves CO_2 solubility of the overall system per unit volume. The CO_2 solubility of the IL mixtures was evaluated by equilibrating each liquid under varying pressures of CO_2 gas at 50°C and measuring the amount absorbed. These results were then fitted to a polynomial curve, and interpolated to account for variance in pressure during measurement. The results indicate that on the practical basis of moles of CO_2 per volume of IL mixture, the $[C_1C_1pyrr]_{0.2}[C_1pyr]_{0.8}[Tf_2N]$ showed comparable absorbance of CO_2 to $[C_6C_1im][Tf_2N]$ at low pressures and up to 8% higher at elevated pressures (Figure 3) and makes it more applicable for warm gas purification. It is suspected that not having long alkyl chain increases the overall ionic nature of the system improving overall CO_2 solubility per unit volume of liquid. Such increased CO_2 solubility is promising for future trials with mixed systems of truncated cations.

Heat capacity

For applications involving heating the ionic liquid, heat capacity determines how much energy will be required. Heat capacity for these samples was measured by DSC at three different temperatures (Figure 4). The heat capacities range from 430 to 621 $J \cdot mol^{-1} \cdot K^{-1}$, with some fluctuation in the general upwards trend with increasing $[C_1C_1pyrr][Tf_2N]$ content. Overall, the heat capacities are lower than that of $[C_6C_1im][Tf_2N]$. The lower heat capacity compared to

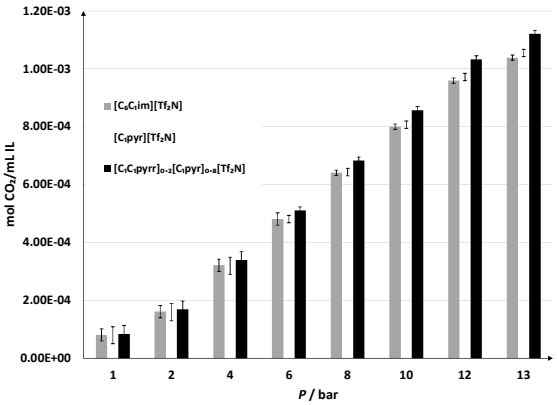

Figure 3. CO_2 sorption of $[C_6C_1im][Tf_2N]$[34], $[C_1pyr][Tf_2N]$, and the best-absorbing binary mixture measured at 50°C and various pressures, interpolated from experimental data. Sorption is shown as moles CO_2 absorbed by a given starting volume of ionic liquid.

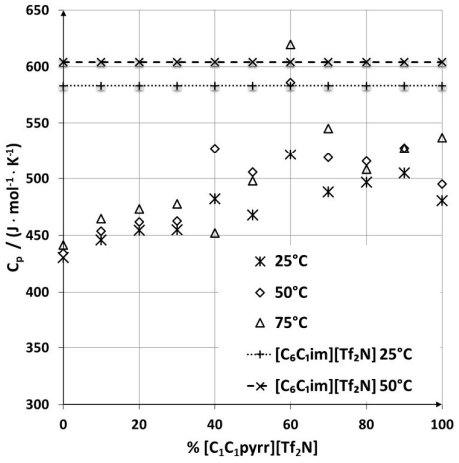

Figure 4. Heat capacities of all samples measured at 25, 50, and 75°C. Data for $[C_6C_1im][Tf_2N]$ at 25 and 50°C is shown for comparison.[18] Error bars are omitted for clarity (Error <1%).

$[C_6C_1im][Tf_2N]$ is most likely due to the fewer intramolecular degrees of freedom in the smaller ionic mixtures.

Conductivity

The electrical conductivity of IL compounds determines their usefulness in electrochemical applications. The three binary combinations (10–30% $[C_1C_1pyrr][Tf_2N]$) that were stable liquids at 50°C were measured for conductivity at this temperature. The results ranged from 11.2 to 12.2 $mS{\cdot}cm^{-1}$, which is a threefold improvement over $[C_6C_1im][Tf_2N]$'s conductivity of 4.1 $mS{\cdot}cm^{-1}$ (Table 1). This could be partially due to the increased charge per unit volume that results from smaller cations, but the dramatic boost suggests other mechanisms are at work as well. The lack of alkyl chains on the cations could reduce aggregation, possibly improving conductivity due to increased mobility. An alternate explanation for the increase in conductivity may be the inability of this system to form any ionic liquid aggregates and nano-domains[25,35] due to the lack of a hydrocarbon chain. Their high conductivity makes these binary mixtures potential candidates for electrochemical applications.

Two properties of these novel ionic liquid mixtures are particularly interesting. First, the conductivity is nearly three times that of $[C_6C_1im][Tf_2N]$ even though the dynamic viscosity is the same within 5%. Second, the solubility of CO_2 is comparable between the mixtures and $[C_6C_1im][Tf_2N]$ with 15% higher density.

Table 1. Data summary for eutectic IL samples compared to [C6C1im][Tf2N]

	$[C_6C_1im][Tf_2N]$	$[C_1pyr][Tf_2N]$	% $[C_1C_1pyrr][Tf_2N]$		
			10	20	30
T_m, °C	-7[9]	45	39	34	33
η, mPa[a]	26[9]	23.9	24.7	25.1	26.2
ρ, $g{\cdot}cm^{-3}$[a]	1.35[11]	1.58	1.57	1.55	1.54
k_H (atm)[a]	46.8	66.5	52.3	47.6	51.7
κ ($mS{\cdot}cm^{-1}$)[a]	4.07	-	11.2	12.2	11.9
C_p ($J{\cdot}mol^{-1}{\cdot}K^{-1}$)[a]	604[18]	434	454	462	463

[a] Measured for liquid at 50°C and ~1 atm

Molecular insights via 2D-IR spectroscopy

To gain a better understanding of the microscopic causes of these macroscopic observations, we used 2D-IR spectroscopy to probe the picosecond dynamics of the mixtures compared with $[C_6C_1im][Tf_2N]$. 2D-IR spectroscopy is a coherent vibrational spectroscopy, which is analogous to 2D NMR spectroscopy. Where 2D NMR correlates nuclear spins, 2D-IR correlates molecular vibrational frequencies. The 2D-IR lineshape encodes the rate at which the local environment changes around a molecule.

Not all molecular vibrations are sufficiently intense to observe in a 2D-IR spectrum; CO_2, however, is an ideal vibrational chromophore for 2D-IR in ionic liquids.[27] The vibrational spectrum of the CO_2 asymmetric stretch depends on local intermolecular interactions such as electrostatics, charge transfer, and hydrogen bonding.

We used the CO_2 asymmetric stretch as a probe for 2D-IR spectroscopy to investigate the differences in the local environment experienced by CO_2 in both $[C_1C_1pyrr]_{0.3}[C_1pyr]_{0.7}[Tf_2N]$ and $[C_6C_1im][Tf_2N]$ (Figure 5). While this experiment has direct motivation from the potential use of these novel ionic liquids for carbon capture, this molecular probe also allowed us to investigate the local motions of the cation and anion, which are important for understanding the differences in conductivity between the ILs, and which CO_2 does not greatly disrupt.The microscopic dynamics in the two ILs are markedly different. Spectra of the CO_2 asymmetric stretch in both ILs start elongated in the diagonal direction (Figure 5A,D), which indicates a distribution of local environments. At 5 ps, the 2D-IR spectrum of the $[C_1C_1pyrr]_{0.3}[C_1pyr]_{0.7}[Tf_2N]$ has become round, indicating that the environment around the CO_2 molecule has randomized (Figure 5B); whereas, the 2D-IR spectrum of $[C_6C_1im][Tf_2N]$ retains some diagonal character (Figure 5E), indicating that the environment around the CO_2 molecules remains similar. In $[C_6C_1im][Tf_2N]$, the spectrum becomes round on a 50 ps time scale (Figure 5F).

This qualitative picture can be quantified by nonlinear least squares fitting of the spectra to third-order response functions.[36] The three important parameters from the analysis are the dephasing time (T_2), which controls the antidiagonal width of the spectra; the inhomogeneous width (Δ) which controls the diagonal width of the spectra; and the spectral diffusion time (τ_c), which controls the rate of change of shape of the spectra. T_2 is related to fast local motions such as hindered rotations (librations), Δ is related to the distribution of different environments, and τ_c is the time scale for relaxation of those initial environments. In $[C_1C_1pyrr]_{0.3}[C_1pyr]_{0.7}[Tf_2N]$, CO_2 shows a marked decrease in τ_c, and an increase in T_2 compared with that seen in

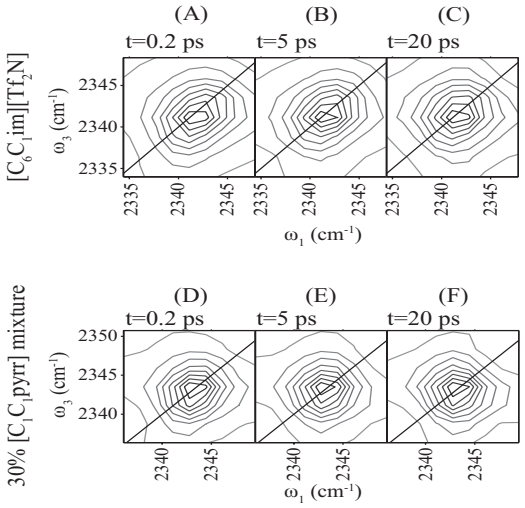

Figure 5. 2D-IR spectra of CO_2 antisymmetric stretch in $[C_6C_1im][Tf_2N]$ and in $[C_1C_1pyrr]_{0.3}[C_1pyr]_{0.7}[Tf_2N]$.

$[C_6C_1im][Tf_2N]$. The difference in τ_c we attribute to differences in the ease of rotations of the ions of CO_2's first solvent shell (see Discussion). The increased dephasing time, T_2, likely results from a narrower distribution of CO_2 frequencies during homogeneous motions, perhaps due to the loss of largely uncharged hexyl chains in the first solvation shell. Δ is similar for the two ILs (Table 2).

Table 2. Comparison of best fit parameters for solvation dynamics of CO_2 in $[C_6C_1im][Tf_2N]$ and $[C_1C_1pyrr]_{0.3}[C_1pyr]_{0.7}[Tf_2N]$, from 2D-IR spectral fitting.

Sample	Δ (cm^{-1})	τ_c (ps)	T_2 (ps)
$[C_6C_1im][Tf_2N]$	1.4±0.1	47±9	2.45±0.03
$[C_1C_1pyrr]_{0.3}[C_1pyr]_{0.7}[Tf_2N]$	1.5±0.1	6±2	3.0±0.2

The most striking spectroscopic difference is the eightfold decrease in τ_c between CO_2 in $[C_6C_1im][Tf_2N]$ and $[C_1pyr]_{0.7}[C_1C_1pyrr]_{0.3}[Tf_2N]$. Previous work has identified that, in a range of imidazolium ionic liquids, τ_c for CO_2 is correlated to the solvent viscosity.[36] CO_2 in $[C_6C_1im][Tf_2N]$, as expected, falls on this trend line. The IL mixture, however, despite a similar viscosity, show much faster relaxation of the local structure around CO_2, as evidenced by τ_c. We hypothesize that the removal of the hexyl chains in the novel mixtures removes steric hindrance to rotational motions of the cation. Therefore, CO_2 can move relatively quickly between different local environments.

This spectroscopic finding also provides insight into a possible molecular mechanism for the increased conductivity seen in $[C_1pyr]_{0.7}[C_1C_1pyrr]_{0.3}[Tf_2N]$ compared to $[C_6C_1im][Tf_2N]$. Under an external potential, the decreased energy barrier to solvent reorientation, described above, should allow easier molecular reorientation to permit ion transport, and thus conduction. This effect, combined with decreased intermolecular friction due to the loss of bulky alkyl chains, and increased charge density (due to decreased IL molar volume), provide a plausible explanation for the increased conductivity. It may be possible to exploit combinations of these mechanisms to guide the design of ionic liquids with high conductivity for electrochemical applications.

Conclusions

By mixing two dissimilar cations with shortened alkyl chains, useful ionic liquids properties can be accessed, and tuned. Mixing of the two compounds increases the mobility of the cation, which leads to greatly increased conductivity, which is promising for electrochemical applications. The removal of the hexyl chain also decreases the heat capacity of the IL, which can be important for variety of thermal applications. Despite increased density, CO_2 solubility remains comparable to that of $[CC_1im][Tf_2N]$, and the mixture of two different cations is able to depress the melting point to below 35°C. The melting point and CO_2 solubility can likely be improved further with experimentation. This approach shows promise as a general strategy to inexpensively optimize the properties of ionic liquids by the mixing of simple salts, rather than complicated synthesis of new ILs.

Acknowledgements

This research was supported by the U.S. Department of Energy's National Energy Technology Laboratory under the contract DE-FE0004000. Part of this work was also supported by ACS PRF Award #53936-DNI6.

Notes and references

1 1P. Wasserscheid and W. Keim, *Angew. Chem. Int. Ed. Engl.*, 2000, **39**, 3772–3789.
2 2J. E. Brennecke and B. E. Gurkan, *J. Phys. Chem. Lett.*, 2010, **1**, 3459–3464.
3 3E. D. Bates, R. D. Mayton, I. Ntai and J. H. Davis, *J. Am. Chem. Soc.*, 2002, **124**, 926–927.
4 4M. Armand, F. Endres, D. R. MacFarlane, H. Ohno and B. Scrosati, *Nat. Mater.*, 2009, **8**, 621–9.
5 5H. B. Nulwala, C. N. Tang, B. W. Kail, K. Damodaran, P. Kaur, S. Wickramanayake, W. Shi and D. R. Luebke, *Green Chem.*, 2011, **13**, 3345.
6 6C. Wang, X. Luo, H. Luo, D. Jiang, H. Li and S. Dai, *Angew. Chem. Int. Ed. Engl.*, 2011, **50**, 4918–22.
7 7G. Cui, J. Zheng, X. Luo, W. Lin, F. Ding, H. Li and C. Wang, *Angew. Chemie*, 2013, **125**, 10814–10818.
8 8E. D. Bates, R. D. Mayton, I. Ntai and J. H. Davis, *J. Am. Chem. Soc.*, 2002, **124**, 926–7.
9 9K. Fukumoto, M. Yoshizawa and H. Ohno, *J. Am. Chem. Soc.*, 2005, **127**, 2398–2399.
10 10B. E. Gurkan, J. C. de la Fuente, E. M. Mindrup, L. E. Ficke, B. F. Goodrich, E. a Price, W. F. Schneider and J. F. Brennecke, *J. Am. Chem. Soc.*, 2010, **132**, 2116–7.
11 11W. Ogihara, M. Yoshizawa and H. Ohno, *Chem. Lett.*, 2004, **33**, 1022–1023.
12 12X. Luo, Y. Guo, F. Ding, H. Zhao, G. Cui, H. Li and C. Wang, *Angew. Chem. Int. Ed. Engl.*, 2014, **53**, 7053–7.
13 13K. A. Fletcher, S. N. Baker, G. A. Baker and S. Pandey, *New J. Chem.*, 2003, **27**, 1706.
14 14P. M. Bayley, A. S. Best, D. R. MacFarlane and M. Forsyth, *Chemphyschem*, 2011, **12**, 823–7.
15 15H. J. Castejón and R. J. Lashock, *J. Mol. Liq.*, 2012, **167**, 1–4.
16 16H. Niedermeyer, J. P. Hallett, I. J. Villar-Garcia, P. a Hunt and T. Welton, *Chem. Soc. Rev.*, 2012, **41**, 7780–802.
17 17G. Chatel, J. F. B. Pereira, V. Debbeti, H. Wang and R. D. Rogers, *Green Chem.*, 2014.
18 18J. M. Crosthwaite, M. J. Muldoon, J. K. Dixon, J. L. Anderson and J. F. Brennecke, *J. Chem. Thermodyn.*, 2005, **37**, 559–568.
19 19J. N. C. Lopes, A. A. H. Padua and K. Shimizu, *J. Phys. Chem. B*, 2008, **112**, 5039–46.
20 20J. L. Anderson, J. K. Dixon and J. F. Brennecke, *Acc. Chem. Res.*, 2007, **40**, 1208–1216.
21 21J. A. Widegren and J. W. Magee, *J. Chem. Eng. Data*, 2007, **52**, 2331–2338.
22 22C. Schreiner, S. Zugmann, R. Hartl and H. J. Gores, *J. Chem. Eng. Data*, 2010, **49**, 4372–4377.

23 23G. J. Maximo, R. J. B. N. Santos, P. Brandão, J. M. S. S. Esperança, M. C. Costa, A. J. A. Meirelles, M. G. Freire and J. A. P. Coutinho, *Cryst. Growth Des.*, 2014, **14**, 4270–4277.
24 24Y. Chen, F. Ke, H. Wang, Y. Zhang and D. Liang, *Chemphyschem*, 2012, **13**, 160–7.
25 25J. N. Canongia Lopes and A. A. H. Padua, *J. Phys. Chem. B*, 2006, **110**, 19586–92.
26 26Y. Wang and G. a Voth, *J. Am. Chem. Soc.*, 2005, **127**, 12192–3.
27 27A. M. Pinto, H. Rodríguez, Y. J. Colón, A. Arce and A. Soto, *Ind. Eng. Chem. Res.*, 2013, **52**, 5975–5984.
28 28Y.-F. Hu, Z.-C. Liu, C.-M. Xu and X.-M. Zhang, *Chem. Soc. Rev.*, 2011, **40**, 3802–23.
29 29J. M. Pringle, P. C. Howlett, D. R. MacFarlane and M. Forsyth, *J. Mater. Chem.*, 2010, **20**, 2056.
30 30C. M. Gordon, J. D. Holbrey, A. R. Kennedy and K. R. Seddon, *J. Mater. Chem.*, 1998, **8**, 2627–2636.
31 31R. D. Chirico, V. Diky, J. W. Magee, M. Frenkel and K. N. Marsh, *Pure Appl. Chem.*, 2009, **81**, 791–828.
32 32K. N. Marsh, J. F. Brennecke, R. D. Chirico, M. Frenkel, A. Heintz, J. W. Magee, C. J. Peters, L. P. N. Rebelo and K. R. Seddon, *Pure Appl. Chem.*, 2009, **81**, 781–790.
33 33M. J. Muldoon, S. Aki, J. L. Anderson, J. K. Dixon and J. F. Brennecke, *J. Phys. Chem. B*, 2007, **111**, 9001–9009.
34 34M. B. Shiflett and A. Yokozeki, *J. Phys. Chem. B*, 2007, **111**, 2070–4.
35 35A. Seduraman, M. Klähn and P. Wu, *Calphad*, 2009, **33**, 605–613.
36 36T. Brinzer, E. J. Berquist, S. Dutta, C. A. Johnson, C. S. Krisher, D. S. Lambrecht, S. Garrett-Roe and Z. Ren, *J. Chem. Phys.*, 2015, **142**, 212425.
37